International Baccalaureate Diploma Program

Extended Essay

Chemistry

Research Topic: Enhancing enzymatic hydrolysis of cotton-based textiles

Research Question:

How does the concentration of Triton X-100 (0%, 0.02%, 0.03%, 0.04%, 0.05%, 0.06%, 0.07%, 0.08% v/v) influence glucose yield from a 48-hour cellulase-mediated cotton-hydrolysis, quantified by DNSA assay?

Word Count: 3987

Table of Contents

1. Introduction

1.1: Personal and Global Relevance

Green-Square Textiles is a non-profit organisation dedicated towards sustainable textile management. Interning there for a few months provided me insights into the pressing issues within the textile industry. Over '92 million tonnes of textiles waste are produced every year', that end up in landfills, leaving a large carbon footprint of 10% global annual carbon emissions (Sanchez, 2023) (Metsola, 2020). Therefore, it is important to redirect textile waste from landfills, for instance via recycling.

1.1.1: Mechanical Recycling

Through internship, I realised that mechanical recycling is the most common method used to recycle textiles, given its low-cost, and minimal environmental impact (Hussain, 2023). This process entails mechanically shredding and tearing apart textiles into yarn or shorter fibre pieces. However, with a shift from retail to cheaper fast-fashion garments (Shah, 2024), mechanical recycling is not a sustainable approach in future.

This is because these garments are of lower quality, meaning mechanical recycling processes cause excessive damage to these poor-quality fibres. Consequently, the overall quality of the end-products, like clothing and footwear, made from these recycled materials, is reduced (Law, 2024).

Thus, to prepare for the shift in textile waste to fast-fashion garments, a better alternative to mechanical recycling should be diversified into, like chemical recycling.

1.1.2: Chemical Recycling

Unlike mechanical recycling which changes textiles' physical structure, chemical recycling uses chemical agents and processes to change textiles' chemical structure (Steilemann, 2023). This generally includes breaking down textiles into its building blocks, and using them to create new products.

For instance, (Taherzadeh, 2009) highlights how cotton-based textiles (CBTs) can be firstly chemically broken down into its constituents (i.e., glucose monomers), and secondly, be fermented into ethanol. Considering ethanol's significance in the energy-market given its ability to reduce vehicular carbon emissions by a substantial 40% (M. Wang et al., 2021), it is therefore important to enhance the chemical conversion of CBTs to ethanol (i.e., increasing efficiency of aforementioned steps).

Given that *Stage 2* (Glucose → Ethanol) depends on the efficiency of *Stage 1* (CBT → Glucose), it is rational to prioritise optimising *Stage 1* first. Consequently, its optimisation increases glucose yield, thereby increasing ethanol yield.

1.2: Research Question

Nevertheless, this essay will determine:

How does the concentration of Triton X-100 (0%, 0.02%, 0.03%, 0.04%, 0.05%, 0.06%, 0.07%, 0.08% v/v) influence glucose yield from a 48-hour cellulase-mediated cotton-hydrolysis, quantified by DNSA assay?

Justification of RQ is below: (pages 5 to 20).

2. Background Theory of Chemical Recycling

Before enhancing *Stage 1*, it is important to first understand it, to help identify its inefficiencies – that would be improved.

2.1: Cotton's Structure

In CBTs, the precursor to glucose is cotton fibre. More specifically, it is cellulose, holding 95% of cotton's composition (Liang et al., 2023). Therefore, it is reasonable to focus on increasing glucose yield from cellulose's chemical breakdown, instead of CBTs'.

Cellulose is a polymer; a long chain of glucose $(C_6H_{12}O_6)$ monomers linked together by 1,4 glycosidic bonds (Figure 1).

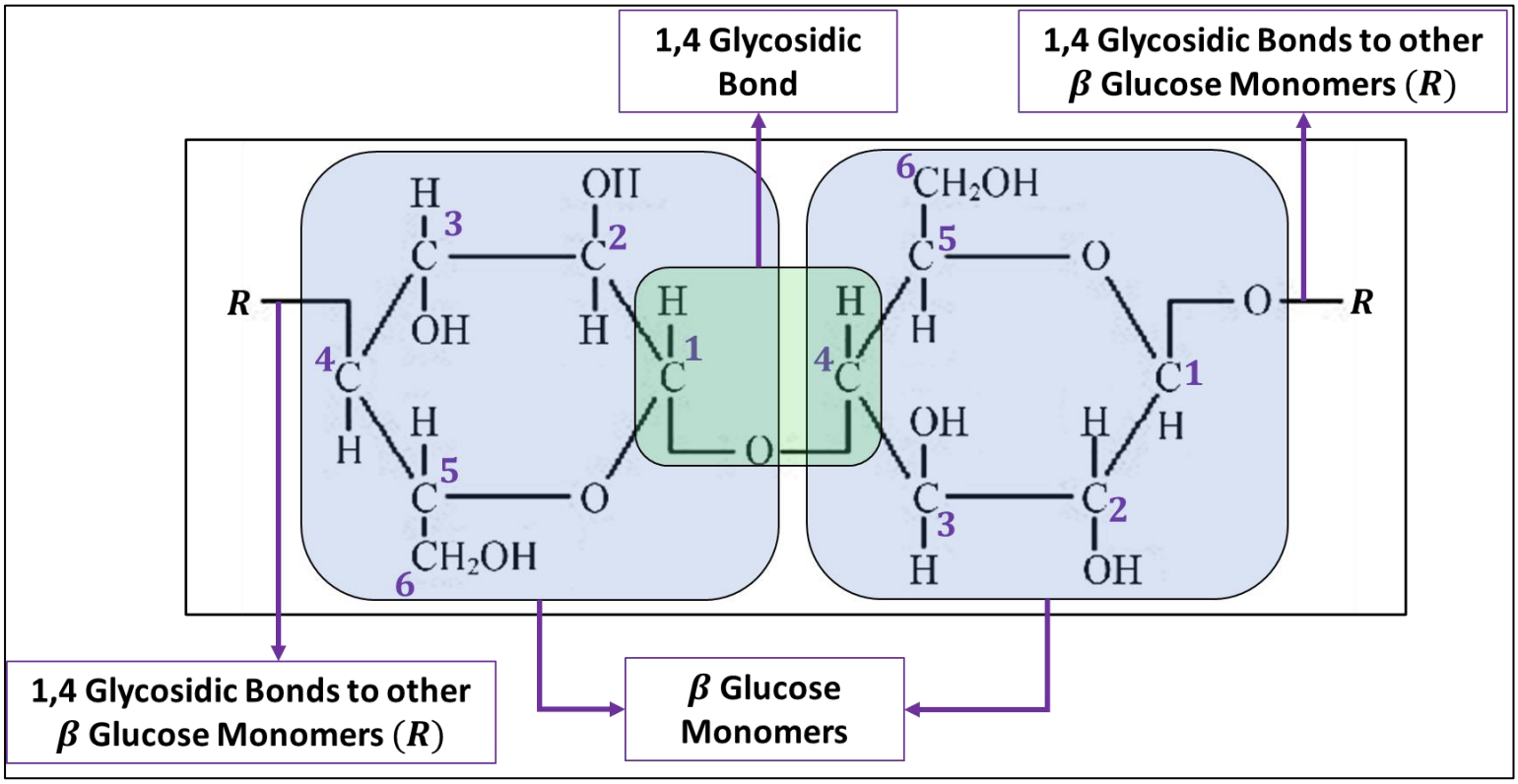

Figure 1: Cellulose's Chemical Structure

Adapted from (Abbas & Li, 2022)

2.2: Yielding Glucose from Cellulose

Thus, cleaving 1,4 glycosidic bonds in cellulose yields glucose (Figure 1) – however possible only through hydrolysis.

2.2.1: Hydrolysis

Cellulose-hydrolysis refers to cellulose's breakdown to its constituent glucose monomers, in the presence of water (Lefers, 2004). However, if cellulose is incompletely hydrolysed, its products include both glucose and cellodextrins (shorter chains of glucose monomers) (Figure 2). Hydrolysing cellodextrins further produces glucose monomers, eventually completing cellulose-hydrolysis.

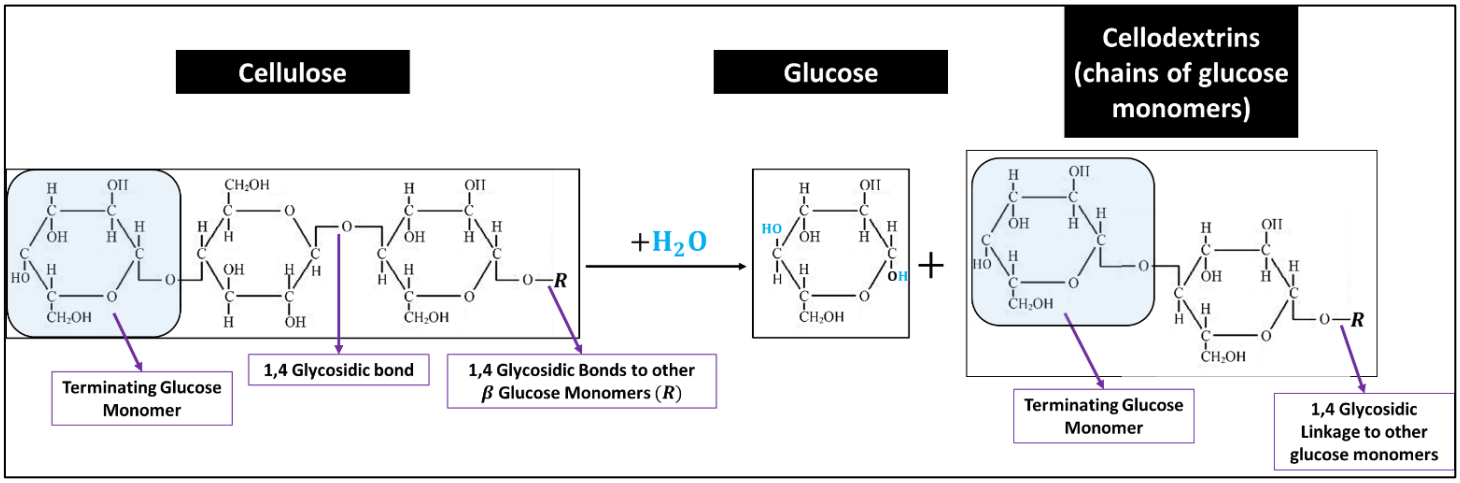

Figure 2: Incomplete Cellulose-Hydrolysis

However, hydrolysis with water is extremely slow (Clark, 2013). It needs to be catalysed to increase glucose yield.

2.2.1.1: Acid/ Base catalysed hydrolysis

One method is acid/base catalysed hydrolysis. This involves subjecting cellulose to acidic (72% sulfuric acid) or alkaline (sodium hydroxide solution) conditions (Mekala et al., 2014) (Kong-Win Chang et al., 2018). However, acid/base

catalysed hydrolysis breaks down more bonds than just 1,4 glycosidic bonds (Yang et al., 2021), meaning final products are even simpler molecules than glucose.

2.2.1.2: Enzymatic Hydrolysis

A preferred alternative is enzymes (biological catalysts) to hydrolyse cellulose, because they are specific, acting on particular substrates to yield specific products. For instance, the enzyme cellulase cleaves only 1,4 glycosidic bonds within cellulose, yielding only glucose monomers upon complete hydrolysis (Greenwood, 2014).

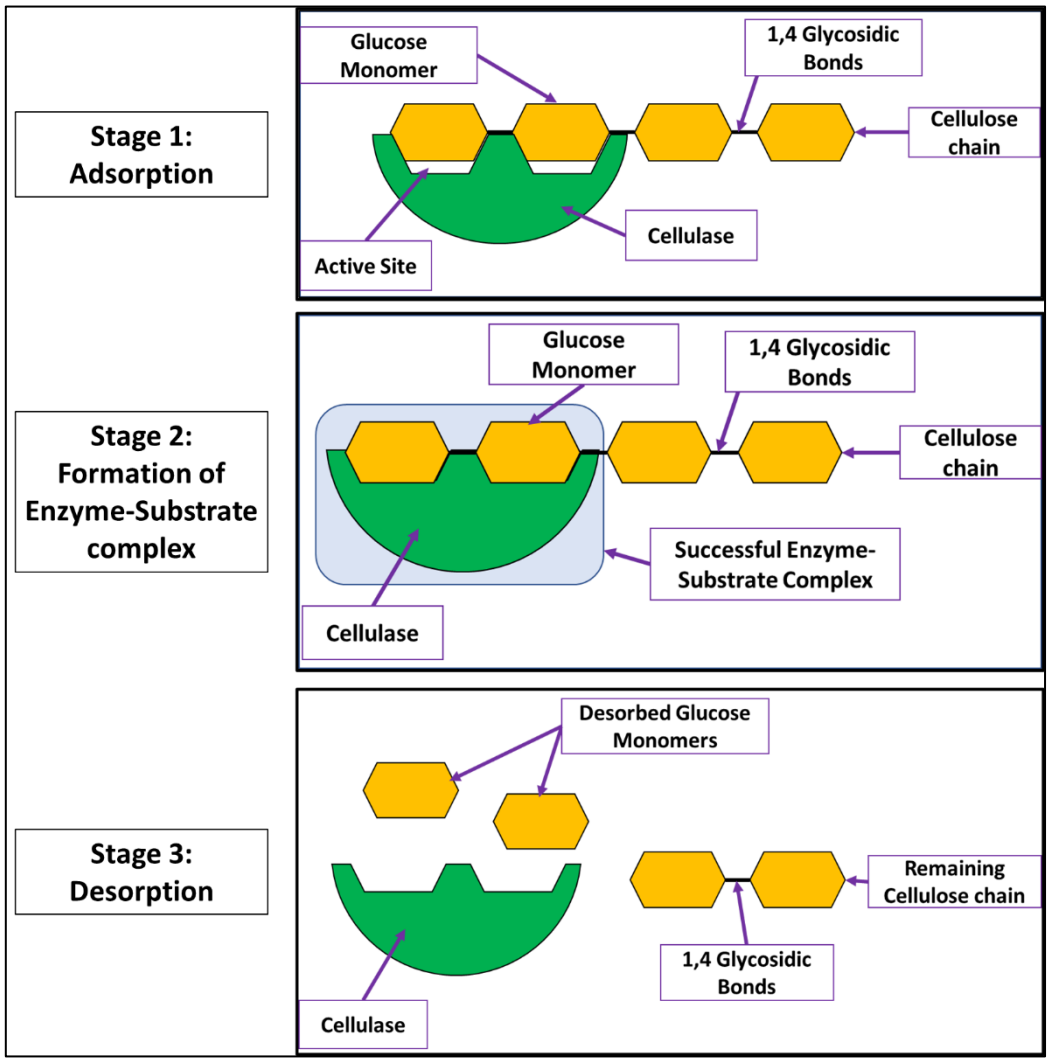

Figure 3: Cellulase-Mediated Cellulose-Hydrolysis

2.2.2: Cellulase-mediated cellulose-hydrolysis

Cellulase hydrolyses cellulose by firstly adsorbing onto the cellulose surface, with its active site coinciding at the 1,4 glycosidic bonds (Figure 3; Stage 1).

In Stage 2 (Figure 3), the Induced Fit Model proposes that the binding of cellulose on cellulase causes conformational changes to cellulase's active site, such that it binds better with cellulose, stabilising the enzyme-substrate complex (Koshland, n.d.). Consequently, cellulase provides an alternative pathway with a lower activation energy, promoting cleavage of 1,4 glycosidic bonds, hydrolysing cellulose into glucose monomers and cellodextrins.

Since these products no longer fit in cellulase's active site, they desorb from cellulase (Figure 3; Stage 3). Desorption ensures that cellulase can adsorb onto other cellulose and cellodextrin substrates, for further hydrolysis, increasing glucose yield.

2.2.2.1: Inefficiencies

However, there are some problems in cellulase-mediated cellulose-hydrolysis.

	Problem	***Effect***
1	Cellulose is sparingly water-soluble. (Gubitosi et al., 2017)	Cellulase is inaccessible to cellulose, reducing cellulose-hydrolysis and glucose yield.
2	Cellulase re-adsorbs onto glucose. (Sánchez-Muñoz et al., 2022)	Glucose inhibits cellulase's interaction with un-hydrolysed cellulose and cellodextrins. With reduced substrate accessibility, less enzyme-substrate complexes are formed, reducing glucose yield.

Table 1: Problems in Cellulase-mediated cellulose-hydrolysis

The most pressing issue is cellulose's sparing water-solubility (Problem 1). Without cellulose dissolving in water, it is inaccessible to cellulase, resulting in no cellulase activity. Whereas, the other problem arises only when cellulase activity is present.

2.2.2.1.1: Cellulose's insolubility in water

Water molecules are polar, because of the partial positive and negative charges on its hydrogen and oxygen atoms respectively. Thus, they dissolve other polar molecules by forming hydrogen bonds (bonds between hydrogen atom of a molecule with a nitrogen, fluorine or oxygen atom of another molecule) with them, pulling them out of their stable structure (Felgenhauer & Khudhir, n.d.).

Despite possessing numerous hydroxyl (-OH) groups capable of forming hydrogen bonds with water molecules (Zuppolini et al., 2022), cellulose remains insoluble in water, because the hydroxyl groups are instead forming hydrogen bonds with either neighbouring cellulose chains (intermolecular) or with linked neighbouring glucose monomers (intramolecular) (Figure 4). Thus, cellulose molecules aggregate to form cellulose fibres, stabilising its structure, preventing its dissolution in water (Burns & Themens, 2014).

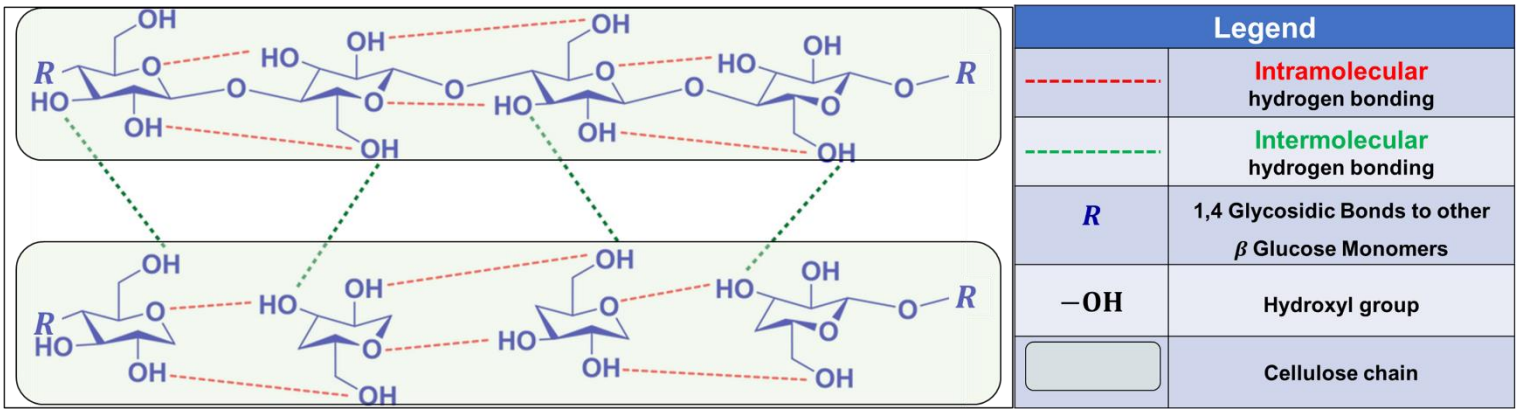

Figure 4: Hydrogen bonding within cellulose

Adapted from (Sharma et. al., 2022)

Therefore, cellulose's water solubility can increase by disrupting these hydrogen bonds.

(Wu et al., 2023) proposes subjecting cellulose to acidic or alkaline conditions. However, this hydrolyses cellulose beyond glucose (Yang et al., 2021), reducing glucose yield; unsuitable. (Swatloski et al., 2002) recommends changing the solvent from water to aqueous ionic liquids (salts that are liquid at room temperature). However, these liquids inactivate cellulase, preventing cellulose-hydrolysis, reducing glucose yield (Pedersen et al., 2019); unsuitable.

Nevertheless, (S. Park et al., 2020) highlights surfactants' ability to increase cellulose's dissolution in water.

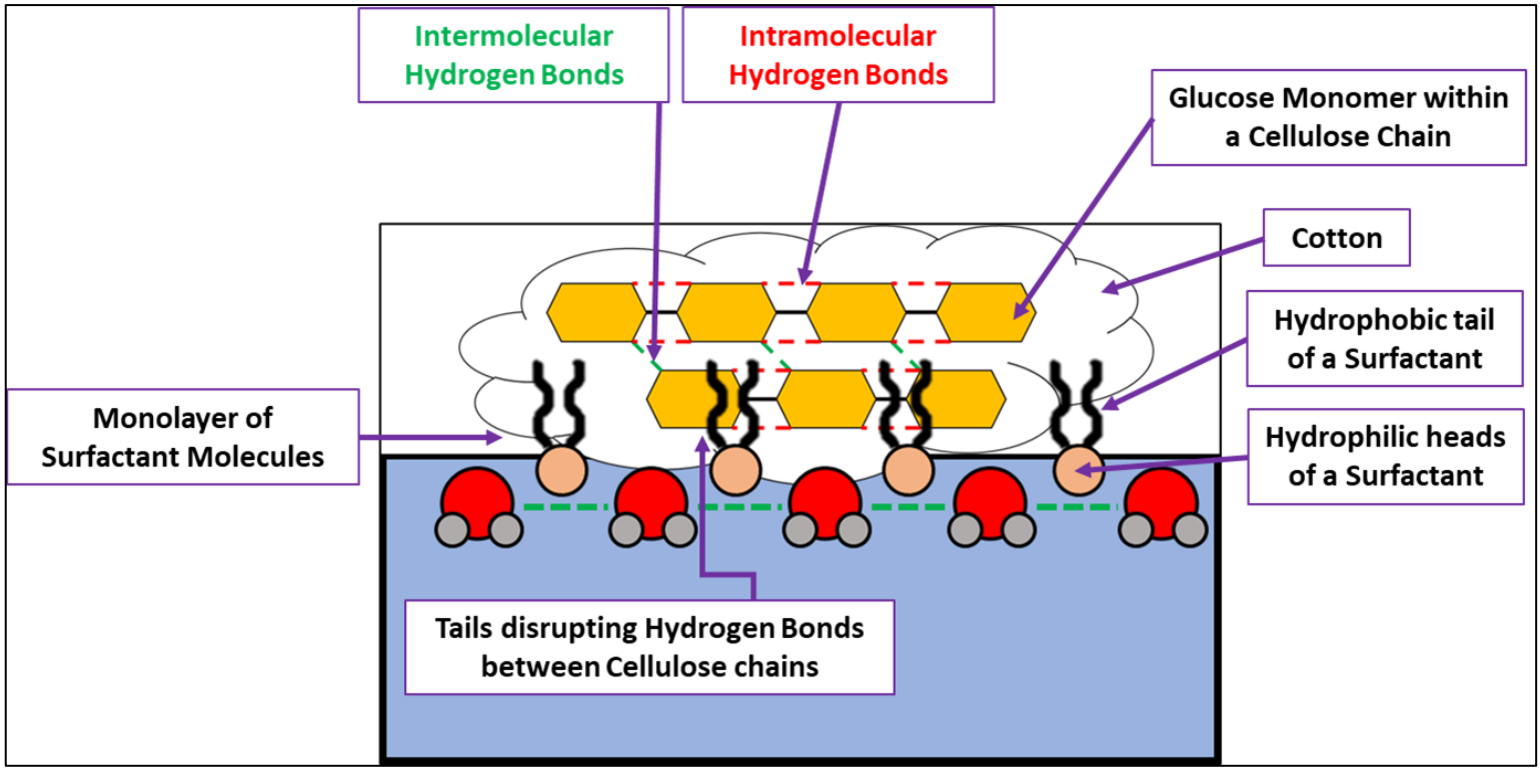

Figure 5: Surfactants in Water

Surfactants are amphiphilic molecules with hydrophilic heads and hydrophobic tails (Ghosh et al., 2020). When added to water, they arrange into a monolayer at the water-cellulose interface (Figure 5). Their hydrophilic heads face the water while the hydrophobic tails extend away from water, into cellulose.

Consequently, the tails weaken the cohesive hydrogen bonding between cellulose chains (Lindman et al., 2021), reducing cellulose's structural stability, enabling water to penetrate it.

The tails also disrupt hydrogen bonding between water molecules at water's surface, promoting their dispersion into cellulose (NCMC, n.d.). Thus, hydroxyl groups within cellulose form stronger hydrogen bonds with the water molecules. Consequently, cellulose dissolves in water.

2.2.2.1.2: Types of Surfactants

However, ionic surfactants are unsuitable to increase cellulose's solubility because their ionic groups reacts and causes conformational changes to cellulase's active site (J. Zhang & Yu, 2017), hindering its catalytic activity.

Therefore, non-ionic surfactants should be used because of their lack of charged groups – they increase cellulose's solubility without compromising its hydrolysis.

As non-ionic surfactants' concentration increases, extent of cellulose's dissolution in water increases. At the critical micelle concentration (CMC), surfactant aggregate to form micelles in water – tiny spheres with surfactants' hydrophobic tails inwards and hydrophilic head outwards (S. Park et al., 2020) (Figure 6).

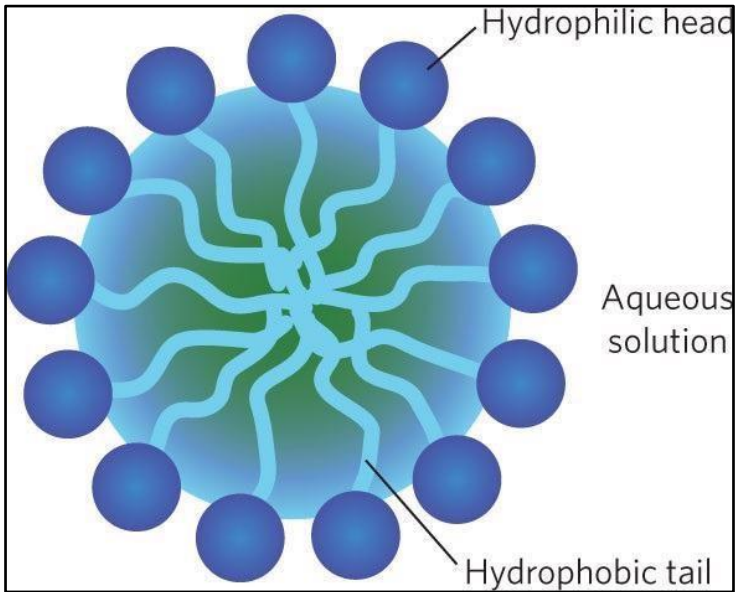

Figure 6: Micelles (Yun, 2021)

At concentrations slightly above CMC, loosely-packed micelles (micelles consisting minimal surfactant molecules) are formed. These micelles increases flexibility of cellulase's active site (Chin & Somasundaran, 2014). This eases its conformational changes required during cellulose-hydrolysis (Page 8), increasing glucose yield.

However, higher non-ionic surfactant concentrations intensify surfactants' hydrophobic interactions with cellulase, reducing cellulase's adsorption onto cellulose, inhibiting its hydrolysis, reducing glucose yield (Z. Wang et al., 2013).

This raises the question of finding ideal concentration of non-ionic surfactant. It needs to be high enough to enable micelle formation while minimising its hydrophobic interactions with cellulase.

In their investigation into enzyme-mediated lignocellulose's (extracted from newspapers) hydrolysis, (J. W. Park et al., 1992) revealed an optimum Triton X-100 [non-ionic surfactant; T100] concentration of 0.05 %v/v (Figure 7) (J. W. Park et al., 1992).

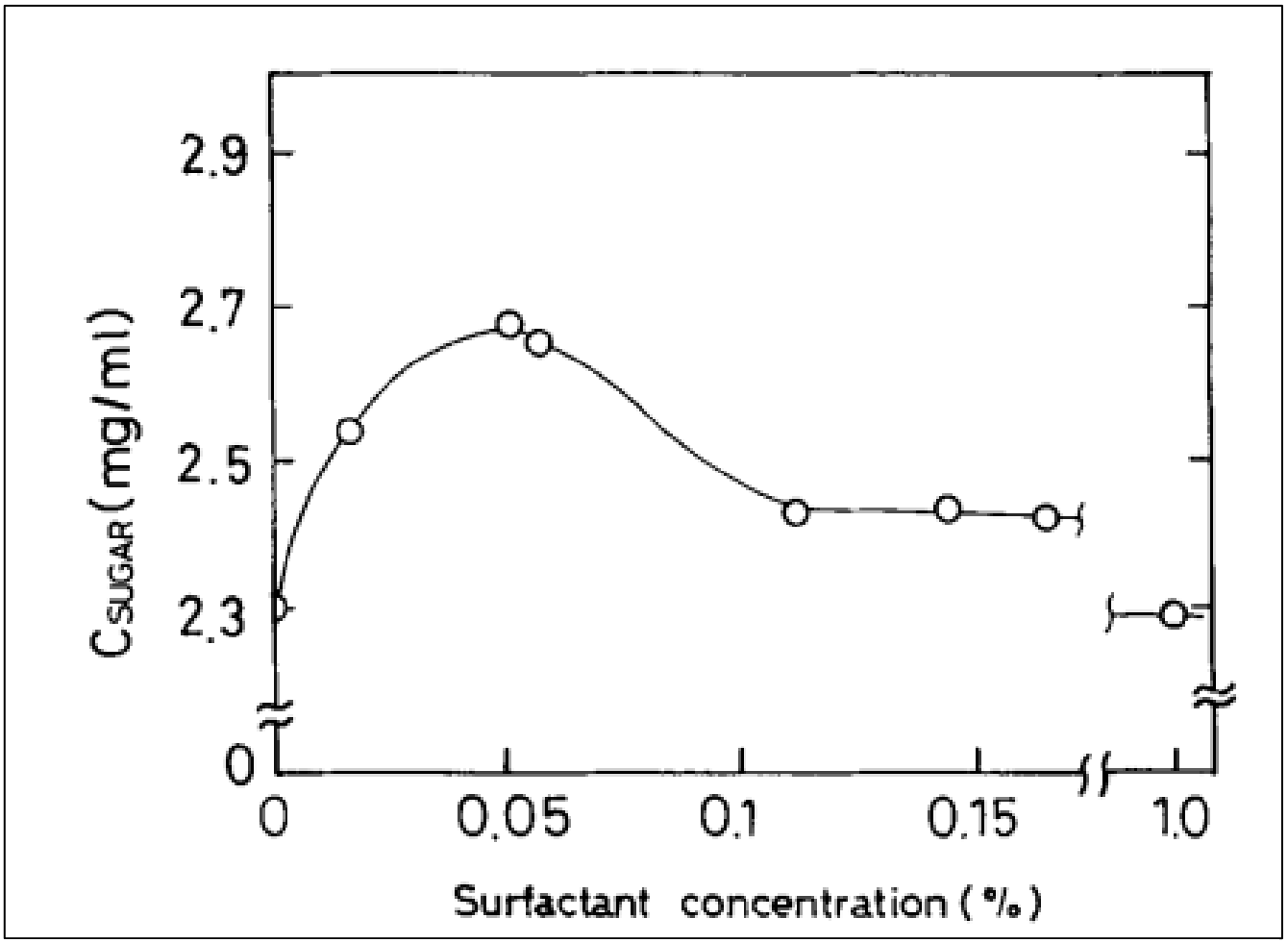

Figure 7: Impact of T100 concentration on sugar concentration from lignocellulose-hydrolysis (J. W. Park et al., 1992)

Given a similar substrate (lignocellulose and cellulose) and a readily available surfactant (T100), it is possible T100's efficiency also extends to CBTs, hence the RQ (Page 4).

2.3: Hypothesis

As T100 concentration increases from 0%v/v to 0.05%v/v (optimal concentration), glucose yield increases, beyond which glucose yield decreases at a decreasing rate.

3. Justification of Methodology

3.1: Replacing CBTs with industrial cotton

Cellulose is the precursor to glucose in CBTs. However, extracting it from CBTs is complex (Costa et al., 2022), thus unfeasible in school laboratories, and cellulose powder is expensive. A cheaper alternative is substituting industrial cotton (used in CBT production) as the substrate, since its composition is mainly cellulose (95%) (Liang et al., 2023).

3.2: Cotton Pre-treatment

To compare with (J. W. Park et al., 1992)'s experiment, a similar procedure is required for a fair comparison. Their experiment involves pre-treating the substrate by air-drying (1 hour at 105℃), to weaken lignocellulose's hydrogen bonds, increasing its water-solubility. Thus, for pre-treatment, cotton is heated in the oven (105℃ for 1 hour). Otherwise, cotton remains clumped despite optimum TX100's presence (0.05%v/v), as observed in preliminary trials (Figure 8).

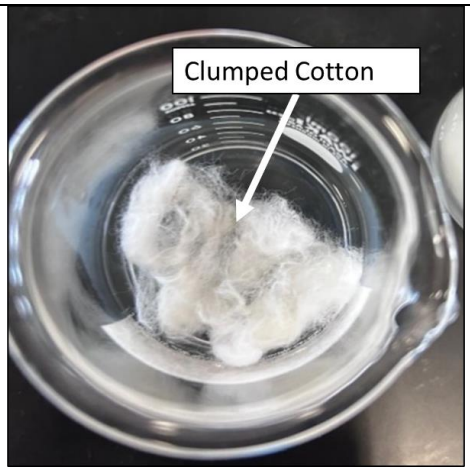

Figure 8: Cotton without pre-treatment (0.05%v/v)

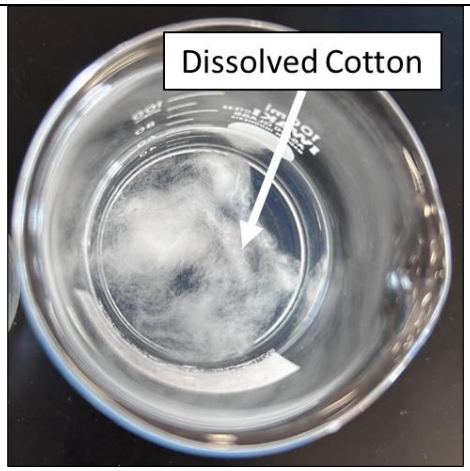

Figure 9: Cotton with pre-treatment (0.05%v/v)

3.3: DNSA Assay Mechanism

To determine glucose yield from cellulase-mediated cellulose-hydrolysis, 3,5-dinitrosalicylic acid reagent (DNSA) is chosen, similar to the literature experiment.

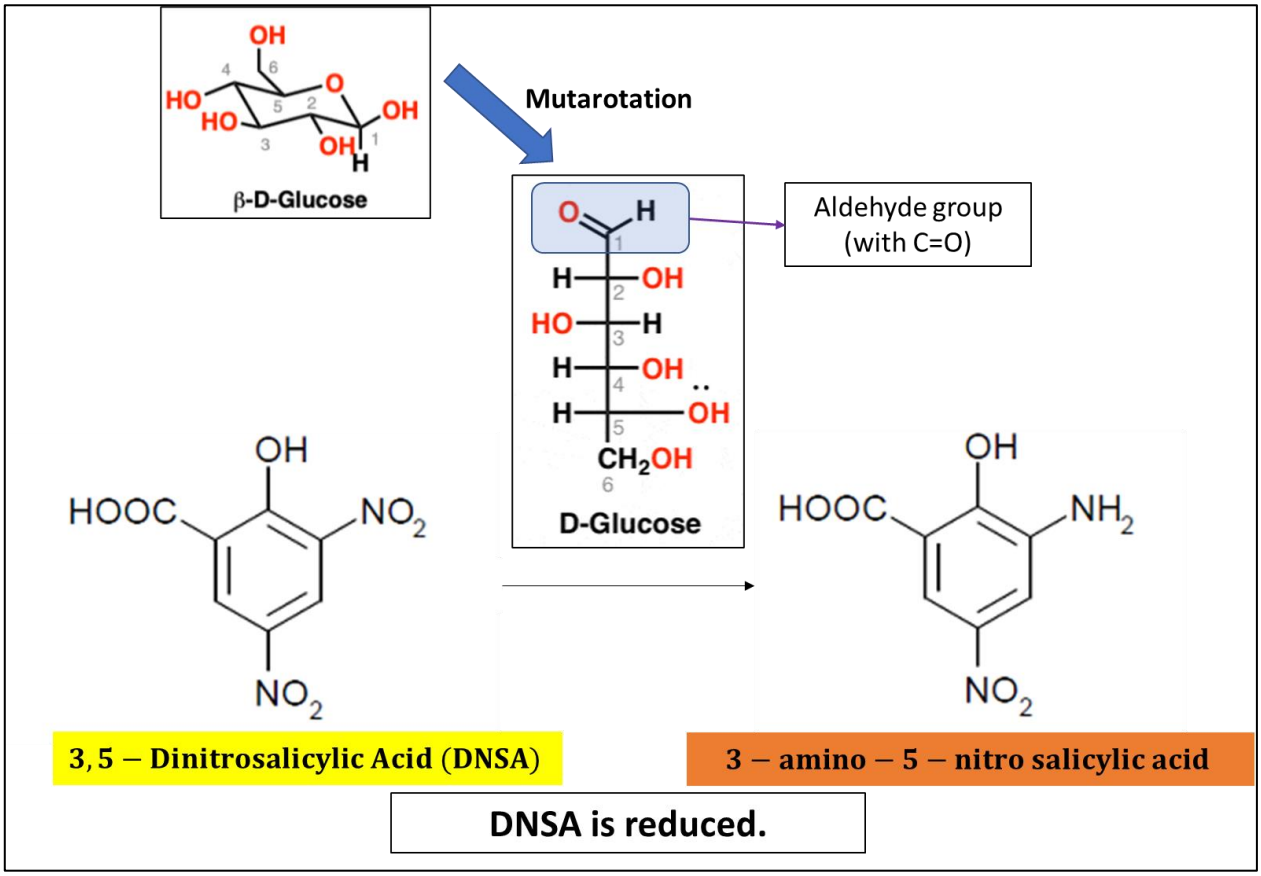

Figure 10: Mutarotation of Glucose and Reducing DNSA (Ashenhurst, 2017)

Adapted from (DNSAinstructions.Pdf, n.d.)

After cellulase-mediated cellulose-hydrolysis, glucose monomers are produced and in water, these monomers undergo mutarotation, changing from a cyclical to a linear structure (Ashenhurst, 2017). The carbonyl group (C=O) in glucose's linear structure reduces DNSA to 3-amino-5-nitro salicylic acid (ANSA), which under alkaline conditions is converted from a yellowish to a reddish-brown coloured complex (*DNSAinstructions.Pdf*, n.d.). Thus, ANSA's concentration ∝ glucose's concentration.

However, colour change is qualitative and only determines the presence of ANSA. Rather, spectrophotometrically analysing the assay quantifies ANSA's concentration, by determining the solution's absorbance of radiation at different wavelengths. A solution's absorbance is linearly proportional to its concentration, but only till absorbance value of 1, according to Beer Lambert's Law (Clark, 2013).

(P. Zhang et al., 2019)'s standard curve illustrates the relationship between an DNSA assay's glucose concentration to its absorbance at 550nm (Figure 11). This is an accurate curve because it was constructed using only absorbance values up to 1.

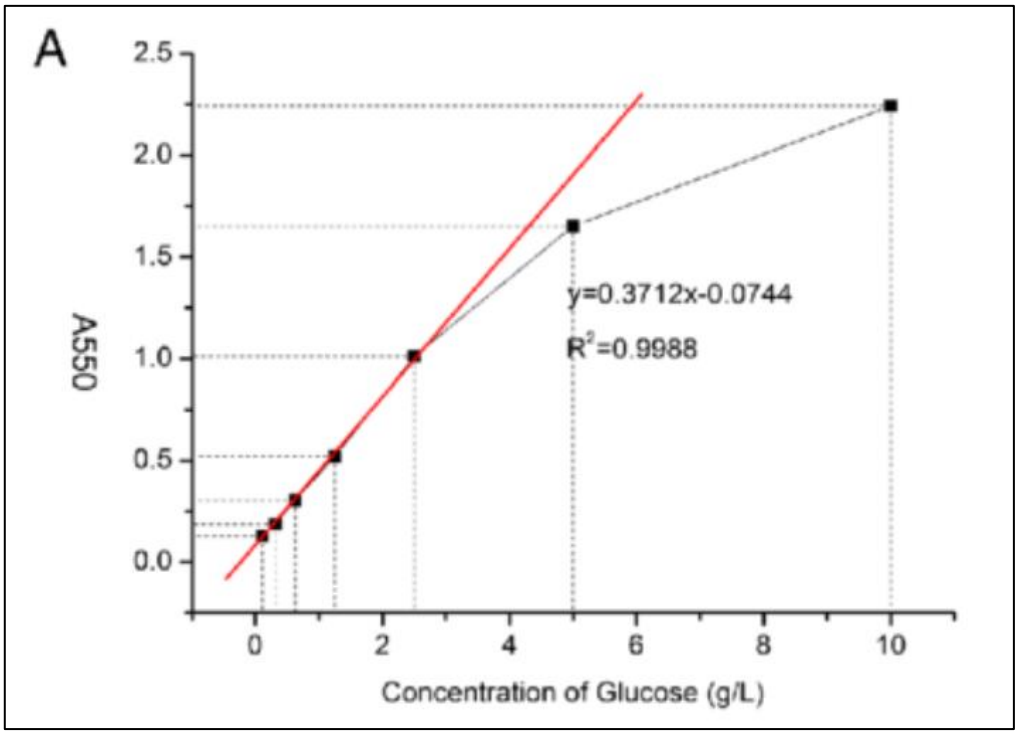

Figure 11: Glucose Standard Curve with DNSA (P. Zhang et al., 2019)

Thus, DNSA-reagent is prepared similar to (P. Zhang et al., 2019), to ensure consistency for accurate spectrophotometric analysis.

3.4: Components and Conditions of Reaction Mixture

3.4.1: Cellulase Mass, pH, Temperature and Heating Duration

In preliminary trials, DNSA assay revealed no glucose yield, even after heat pre-treatment and literature optimum T100 concentration (0.05%v/v). Thus, cellulase activity had to be further maximised.

(Block, n.d.) suggests an optimum cellulase mass of 0.200g, for maximum catalytic rate.

Also, Cellulase performs optimally at pH6, and at 50°C (El-Sersy et al., 2010) (Pardo & Forchiassin, 1999). Therefore, pH6 buffer was added to the reactant mixture, which is placed in the oven at 50°C, for 48-hours (reaction period).

The literature experiment suggested a 22-hour reaction period, but from preliminary trials, it yielded indistinguishable amounts of glucose. Therefore, it had to be increased. From preliminary trials, 48 hours showed an optimal balance; sufficiently long to produce quantifiable glucose yields, yet short enough to preserve distinguishable differences across varying T100 concentrations.

Otherwise, even longer durations would result in near-complete cellulose-hydrolysis, yielding maximum glucose levels across all set-ups regardless of T100 concentration, falsely implying T100 concentration does not influence glucose yield.

3.4.2: T100 concentrations

T100's micelles increase cellulase activity (Page 12). To maintain consistency, across all trials, T100's concentration must exceed its critical micelle concentration (CMC), the concentration at which micelles form.

8 data-points are needed to plot a reliable curve, given the parabolic relationship between T100 concentration and glucose yield (Figure 7). Thus, calculations are made to determine the varying T100 concentrations for the 8 data-points.

A 50ml reaction volume has been selected for cellulase-mediated cellulose-hydrolysis' process. This volume ensures that even minimal concentrations of glucose, resulting from the hydrolysis, are sufficiently concentrated, leading to distinguishable absorbance values in DNSA assay.

$$\text{CMC of T100} = 2.2 \times 10^{-4}\text{M}$$

(*T8532pis.Pdf*, n.d.)

Thus, in a 50mL reaction mixture, a minimum of $\frac{2.2\times10^{-4}}{1000} \times 50 = 1.1 \times 10^{-5} mol$ of T100 is required.

T100's chemical formula is $\text{C}_{14}\text{H}_{22}\text{O}(\text{C}_2\text{H}_4\text{O})_\text{n}$, where *n* = length of T100's polyethene oxide chain, which on average is **10** (*31836001.Pdf*, n.d.).

$$\therefore M_{Triton} = (12.01 \times 14) + (1.01 \times 22) + 16.00 + [(12.01 \times 2) + (1.01 \times 4) + 16.00)] \times \mathbf{10}$$

$$= 646.96 g mol^{-1}$$

$$\rho_{T100} = 1.06 g cm^{-3}$$

$$\therefore 1\ mol\ of\ T100 = \frac{646.96g}{1.06 g cm^{-3}} = 610 cm^3\ of\ T100$$

$$CMC_{T100} = 1.1 \times 10^{-5}\ mol\ of\ T100 = 0.00671 cm^3\ of\ T100$$

Thus, to exceed T100's CMC, more than $0.00671 cm^3$ of T100 must be present in the $50 cm^3$ reaction mixture, corresponding to a '$\%v/v$' greater than $0.0134\%v/v$.

For simplicity, let minimum T100 concentration be $0.02\%v/v$. However, measuring $0.02\% \times 50cm^3 = 0.01cm^3$ of T100 is difficult using either a pipette or a burette, since they are not calibrated to transfer such volumes. Thus, a diluted T100 solution is created by adding $1cm^3$ of T100 to $99cm^3$ of water in a $100cm^3$ volumetric flask. Consequently, $1cm^3$ of this diluted solution contains $0.01cm^3$ of T100 solution.

Thus, these are the volumes of respective liquids for each T100 concentration:

T100 concentration (%v/v)	Volume of diluted T100 solution (cm^3)	Volume of pH6 buffer (cm^3)	Reaction volume (cm^3)
0	0	50	50
0.02	2	48	50
0.03	3	47	50
0.04	4	46	50
0.05	5	45	50
0.06	6	44	50
0.07	7	43	50
0.08	8	42	50

Table 2.1: Liquid Components of Reaction Mixture at differing T100 concentrations

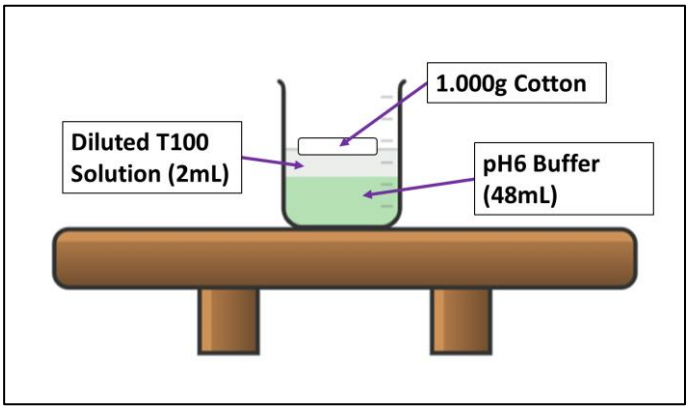

Figure 12: Liquid components of Reactant mixture at 0.02%v/v

Table 2: Calculations to determine the differing T100 concentrations

3.5: Measuring the reaction mixture's volume after hydrolysis

Despite fixed starting volumes of 50mL, final volumes varied in each beaker after the 48-hour hydrolysis period in the oven, indicating varying rates of evaporation. Attempts to standardise the exposed surface area of the reactant mixture to oven's internal-environment using equal numbered and sized holes on the parafilm-sealed beakers were also insufficient.

Thus, comparing glucose concentrations is no longer feasible, as two or more solutions could have identical amounts of glucose but differ in volume due to evaporation. Consequently, the solution with the reduced volume would falsely appear to have a higher glucose concentration, despite the actual glucose content being the same. Nevertheless, using the formula 'Concentration x Volume = Mass', determining glucose yield would rely on mass rather than concentration, preventing the impact of differing volumes.

4. Methodology

4.1: Variables

Types of Variables	Variable Measured	Methodology	Rationale
Independent Variable	T100's $'\%v/v'$ in reactant mixture	Each reactant mixture contains differing volumes of diluted T100 solution	From hypothesis, varying T100's '$\%v/v$' influences glucose yield.
Dependent Variable	Absorbance of DNSA Assay	*Spectrophotometry,* under *Procedure*	The hypothesis suggests that T100's '$\%v/v$' affects glucose yield from hydrolysis, impacting glucose's concentration quantified by the DNSA assay. Figure 11 also illustrates a positive correlation between glucose concentration and DNSA assay's absorbance, indicating T100's '$\%v/v$' affects DNSA assay's absorbance.

Table 3: Independent and Dependent Variables

Type of Variable	Variable to be controlled	Method of Control	Rationale
Controlled Variables	Mass of cotton per trial	Compress the cotton to eliminate trapped air, ensuring the measured mass reflects only the cotton's weight. Each piece of cotton should be only 1.000g.	Cotton's porous structure traps air, has mass. Therefore, cotton's measured mass is higher than its true mass, reducing reliability of results. For a fair comparison with (J. W. Park et al., 1992), cotton mass is kept at 1.000g, similar to their experiment's substrate mass.
	Heating Duration (Pre-treatment)	*Cotton Pre-treatment,* under *Procedure*	Longer heating durations further weaken intermolecular hydrogen bonds in cellulose, increasing its solubility in water. Consequently, cellulose becomes more readily available to cellulase, increasing glucose yield, preventing T100's '$\%v/v$' from being the only independent variable.
	Heating Duration (Hydrolysis)	Ensure reactant mixture stays in the oven for only 48 hours. After which, heat the reactant mixture at 100℃ for 1 minute, to denature cellulase, hence stopping cellulase-mediated cotton-hydrolysis.	Longer heating durations result in greater cellulase-mediated cotton hydrolysis, increasing glucose yield, preventing T100's '$\%v/v$' from being the only independent variable. 100℃ is chosen because higher temperatures degrade glucose (Alonso-Riaño et al., 2024), reducing glucose yield.
	Amount of cellulase	Cellulase should be from the same origin (Aspergillus Niger).	Cellulase from A. Niger was used since it was readily available. Only such cellulase should be used because those of differing origins catalyse cellulose at differing rates,

Type of Variable	Variable to be controlled	Method of Control	Rationale
		Only 0.200g of cellulase is added to reactant mixture, to enable maximum catalytic rate (Block, n.d.).	yielding differing amounts of glucose (Bilal et al., 2014). Mass of cellulase is fixed at 0.200g because differing concentrations affects glucose yields, until saturation concentration (Robinson, 2015). Such factors prevent T100's '$\%v/v$' from being the only independent variable.

Table 4: Controlled Variables

4.2: Apparatus and Chemicals

Apparatus	Quantity	Uncertainty/ Remarks
Burette	1	±0.05mL
Graduated Pipette	2	±0.02mL
Pipette Filler	2	-
100mL Volumetric Flasks	2	±0.1mL
50mL Measuring Beakers	8	±2.5mL
Parafilm	1 Roll	-
Electronic Weigh Balance	1	±0.001g
Weighing Boats	2	-
Kettle	1	-
Visible Light Spectrophotometer	1	±0.0001Au
Cuvette	4	-
Boiling Tubes	8	-
Plastic Droppers	2	±0.5mL
Spatula	2	-

Table 5: Apparatus

Chemical	Concentration	Mass/Volume
Triton X-100 (T100)	-	2mL
Deionised Water	-	1L
DNSA pellets	-	1g
Sodium Potassium Tartrate pellets	-	30g
Sodium Hydroxide solution	2M	20mL
pH6 Buffer	-	1.5L

Table 6: Chemicals

4.3: Procedure

Phase A: Preparations

A. Preparing diluted T100 Solutions
   1. In a 100mL volumetric flask, pipette 1mL of T100 solution.
   2. Fill the flask with water up to the 100mL mark, with a burette.
   3. Shake the solution well. Let it rest till the bubbles subside.
   4. Repeat Steps 1 to 3, to dilute another 100mL of T100 solution.

A. Cotton Pre-treatment
   1. Compress each piece of cotton to remove trapped air, ensuring measured mass accurately reflects the cotton's weight, standardised at 1.000g per piece.
   2. Prepare 24 pieces of cotton, each flattened into a square shape.
   3. Heat the cotton pieces in an oven at 100℃ for 1 hour.

A. Preparing DNSA (P. Zhang et al., 2019)
   1. In a 250mL volumetric flask, dissolve 1.000g of DNSA and 30.000g of sodium potassium tartrate in 30.00mL of deionised water (transferred via burette).
   2. When the solution turns milky yellow in colour, add 20.00mL of 2M NaOH (transferred via pipette).

3. When the solution turns transparent yellowish-orange in colour, add 100.00mL of deionised water (transferred via burette).

Phase B: Cellulase-Mediated Hydrolysis

B. Preparing Reactant Mixtures
   1. In each of the eight 50mL measuring beakers, add specified volumes of pH6 buffer and diluted T100 solutions, as per Table 2.1 (Page 19).
   2. Using an electronic mass balance, weighing boat and spatula, measure and add 0.200g of cellulase powder to each of the reactant mixtures.
   3. Add 1 piece of squarely-flattened, with similar dimensions, pre-treated cotton into each reactant mixture.
   4. Cover each beaker with parafilm, making 4 holes in the covering to minimise evaporation of reaction mixture.
   5. Place the set of 8 reactant mixtures in an oven set to 50℃ for 48 hours.

B. Stopping Cellulase-Mediated Hydrolysis
   1. After 48 hours, heat the reactant mixture at 100℃ for 1 minute, to denature cellulase, and stop cellulase-mediated hydrolysis.

Phase C: Determining Glucose yield

C. Centrifuge
   1. Transfer the reaction mixture into centrifuge tubes.
   2. Centrifuge each of these tubes at 6000rpm for 10min in a centrifuge.

C. Spectrophotometry
   1. Transfer the supernatant from the centrifuged reaction mixture into a burette to determine its volume.
   2. Boil 100mL of water, and pour it into a beaker.
   3. In a boiling tube, mix 0.3mL of DNSA with 0.3mL of the supernatant from the centrifuged reactant mixture, and 3mL of 2M NaOH (which provides an alkaline environment for the reduction of DNSA).
   4. Stand the boiling tube in the beaker of freshly boiled water for 10 minutes to heat the mixture.
   5. Transfer the diluted mixture into a cuvette.
   6. Measure and record the absorbance at 550nm using a spectrophotometer.

Repeat Phases B and C, 2 more times to collect another 2 data-sets.

4.4: Risk Assessment

4.4.1: Safety Precautions

Chemical	GHS Safety Pictogram	Precautions
3,5-dinitrosalicylic acid (*MSDS-35DINITROSALICYLIC-ACID-CASNO-609-99-03481-EN.Pdf*, n.d.)	 Irritant	Wear lab coat, gloves and goggles. Wash exposed skin thoroughly after handling. Avoid consumption
Triton X-100 (T100) (*T8532pis.Pdf*, n.d.)	 Toxic	
Sodium Hydroxide (2M) (*SDB-9356-IE-EN.Pdf*, n.d.)	 Corrosive	
Sodium Acetate (pH6 Buffer) (*Octet-Sodium-Acetate-Buffers-Datasheet-18-1068-18-1069-18-1070-En-Uk-I-Sartorius-Pdf-137254--Data.Pdf*, n.d.)	 Irritant	

Table 7: Safety Precautions for Chemicals

4.4.2: Environmental guidelines

Triton X-100 (T100) should be disposed as hazardous waste, as it has long lasting environmental damage (*T8532pis.Pdf*, n.d.).

5. Data

5.1: Qualitative Data

1. With increasing T100 '$\%v/v$', the cotton within reactant mixture appeared increasingly fragmented, highlighting a greater extent of dissolution in water.

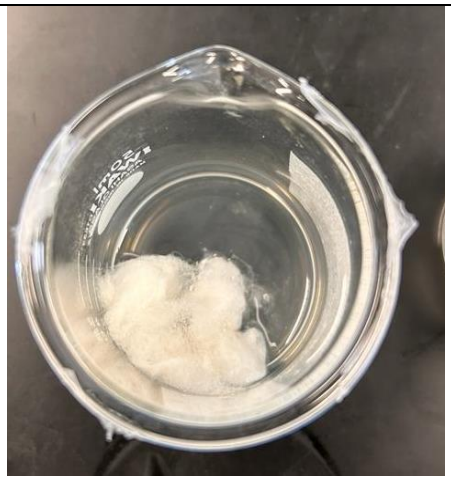		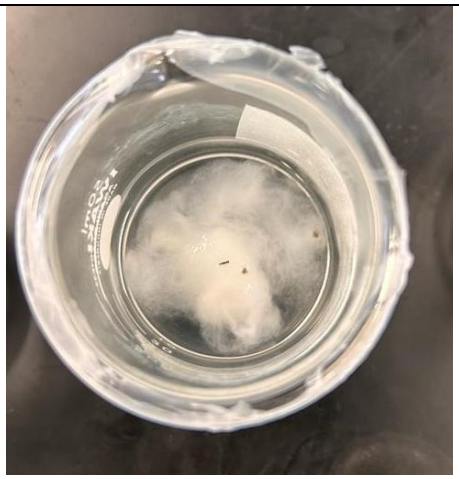
Figure 13: Cotton's Dissolution in 0%v/v T100 reactant mixture after 5min	*Figure 14: Cotton's Dissolution in 0.04%v/v T100 reactant mixture after 5min*	*Figure 15: Cotton's dissolution in 0.08%v/v T100 reactant mixture after 5 minutes*

2. Despite same initial volume, heating conditions and duration, final volumes of reaction mixtures differed, indicating their differing evaporation rates within the oven.

5.2: Quantitative Data

Let Q = T100's percentage volume concentration and M = mass of glucose yield.

5.2.1: Raw Data

Q / %v/v	Data-set 1		Data-set 2		Data-set 3	
	Absorbance at 550nm	Volume /mL $(\pm 0.05mL)$	Absorbance at 550nm	Volume /mL $(\pm 0.05mL)$	Absorbance at 550nm	Volume /mL $(\pm 0.05mL)$
0	0.1421	32.58	0.1459	32.01	0.1135	29.64
0.02	0.1310	36.14	0.1206	34.26	0.1047	35.23
0.03	0.1389	36.54	0.1176	36.74	0.1670	33.02
0.04	0.1374	33.29	0.1463	35.32	0.1330	34.01
0.05	0.1533	35.92	0.1783	32.16	0.1261	37.49
0.06	0.1500	36.38	0.1600	36.42	0.1400	32.91
0.07	0.1512	37.21	0.1567	33.29	0.1070	34.48
0.08	0.1166	36.93	0.1364	35.21	0.1148	35.31

Table 8: Raw Data

5.2.2: Processed Data

Q / %v/v	ΔQ / %v/v	M_1/g	M_2/g	M_3/g	M_{avg}/g	ΔM/g
0	0	0.019	0.018	0.015	0.017	0.002
0.02	0.03	0.020	0.018	0.017	0.018	0.002
0.03	0.05	0.021	0.019	0.016	0.019	0.003
0.04	0.06	0.019	0.021	0.019	0.020	0.001
0.05	0.07	0.022	0.022	0.020	0.021	0.001
0.06	0.09	0.022	0.023	0.019	0.021	0.002
0.07	0.1	0.023	0.021	0.017	0.020	0.003
0.08	0.1	0.019	0.020	0.018	0.019	0.001

Table 9: Processed Data

5.2.3: Sample Calculations

Objective	Steps
ΔQ *Uncertainty in T100's concentration*	**Dilution Titration** When creating the diluted T100 solution (Page 19), 1mL T100 was transferred using a graduated pipette ($\pm 0.2\text{mL}$), and 99mL water measured using a burette ($\pm 0.05\text{mL}$). 2 readings were taken to determine water's 99mL, hence its uncertainty doubles. $$\therefore \%\Delta Q_1 = \frac{0.02}{1} \times 100\% + \frac{0.05 \times 2}{99} \times 100\% = 2.10\%$$ **Reactant Mixture Preparation** For $Q = 0.02\ \%v/v$, 2mL diluted T100 solution was transferred using a graduated pipette ($\pm 0.2\text{mL}$), 48mL pH6 buffer with a burette ($\pm 0.05\text{mL}$), for which its uncertainty doubles as 2 readings were taken. *Let V = volume of solution.* $$Q = \frac{\text{Volume of T100}}{\text{Volume of T100} + \text{Volume of pH6 Buffer}}$$ $$\frac{\Delta Q}{Q} = \frac{\Delta V_t}{V_t} + \frac{\Delta V_t + \Delta V_p}{V_t + V_p}$$ $$\therefore \Delta Q = Q\left(\frac{\Delta V_t}{V_t} + \frac{\Delta V_t + \Delta V_p}{V_t + V_p}\right) = Q\left[(\%V_t)(V_t) + \left(\%V_t + \%V_p\right)\left(V_t + V_p\right)\right]$$ $$\%\Delta V_t = 2.10\% + \frac{0.02}{2} \times 100\% = 3.10\%$$ $$\%\Delta V_p = \frac{0.05 \times 2}{48} \times 100\% = 0.208\%$$ $$\therefore \Delta Q = 0.02[(3.10\%)(2) + (3.10\% + 0.208\%)(50)] = 0.03(1\ s.f.)$$

M_1 *Mass of glucose yield, from Data-set 1*	Figure 11's equation '$y = 0.3712x - 0.0744$' highlights glucose solution's concentration (*x*) to respective DNSA Assay's Absorbance (*y*). Rearranging the equation: $$x = \frac{y + 0.0744}{0.3712}$$ At $Q = 0.02\ \%v/v$, $y = 0.1310$. $$\therefore x = \frac{0.1310 + 0.0744}{0.3712} = 0.55 gL^{-1}$$ At $Q = 0.02\ \%v/v$, volume of glucose solution (V_g) = $36.14\times 10^{-3}L$ $$M_1 = x \times V_g = 0.55 \times (36.14 \times 10^{-3}) = 0.020g(2.s.f)$$
M_{avg} *Average mass of glucose yield*	M_2 and M_3 are calculated similar to M_1. $$M_1 = 0.020g$$ $$M_2 = 0.018g$$ $$M_3 = 0.015g$$ M_{avg} is calculated by taking the average of these 3 results: $$M_{avg} = \frac{M_1+M_2+M_3}{3}.$$ $$\therefore M_{avg} = \frac{0.020 + 0.018 + 0.017}{3} = 0.018$$
ΔM *Uncertainty of glucose yield's mass*	Using the half-range method '$\Delta M = \frac{M_{max}-M_{min}}{2}$', $$\Delta M = \frac{0.020 - 0.017}{2} = 0.002\ (1s.f.)$$

Table 10: Sample Calculations

6. Analysis

6.1: Regression of Processed Data

Power regression models increase in accuracy as higher powers are included; but they are ineffective in illustrating underlying theoretical concepts like in Figure 7.

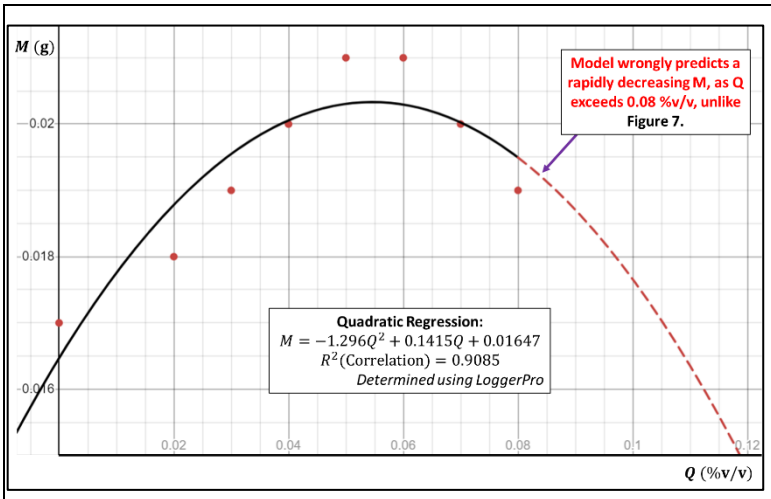

Figure 16: Quadratic Regression

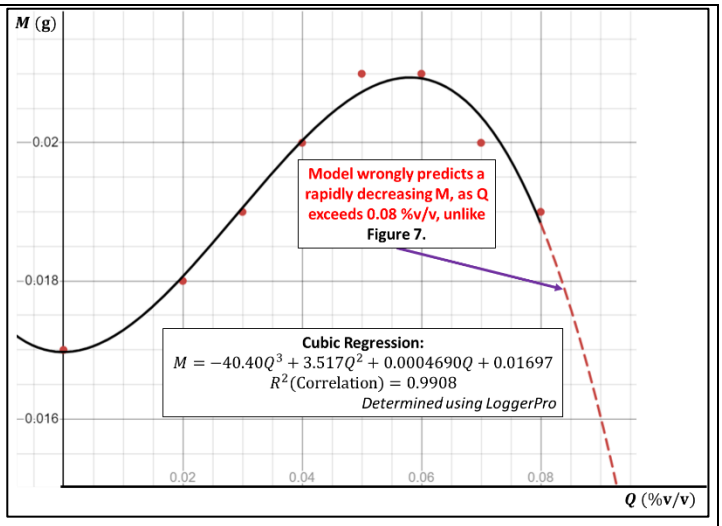

Figure 17: Cubic Regression

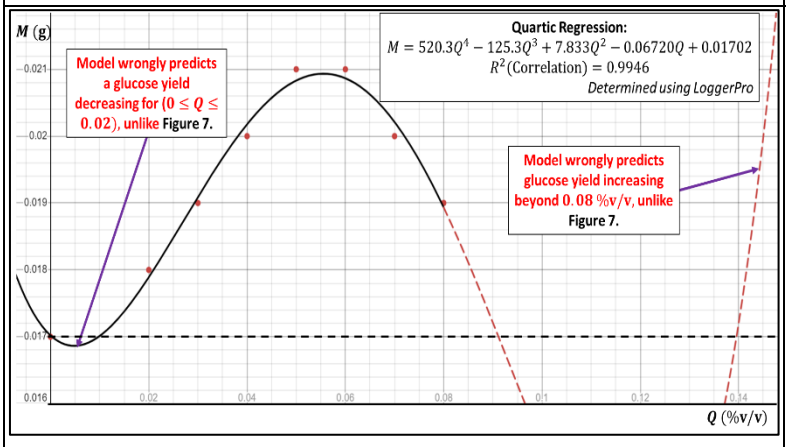

Figure 18: Quartic Regression

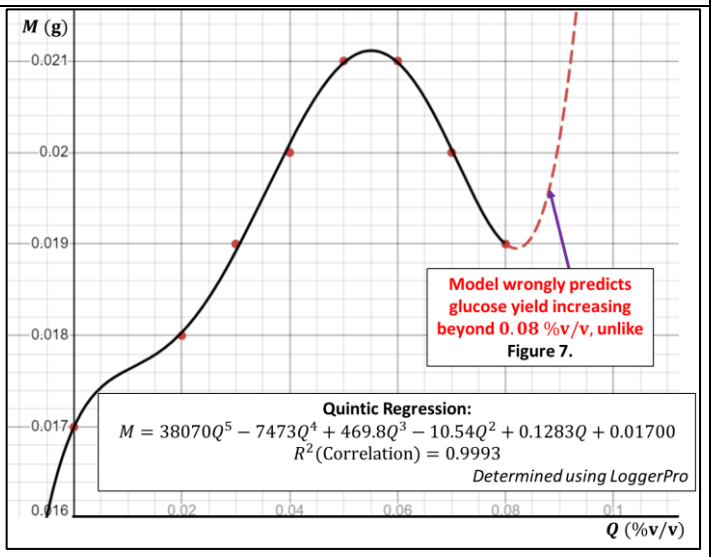

Figure 19: Quintic Regression

Table 11: Power-series Regressions

Thus, gaussian regression of *M* against *Q* is a better alternative (Figure 20), since it is indicative of theory and literature (Figure 7) – decrease in $\boldsymbol{M}$ at a decreasing rate beyond optimum T100 percentage volume concentration ($\boldsymbol{Q_{opt}}$). Given its high R^2 value of 0.9983, the gaussian regression perfectly represents the correlation between *Q* and *M.* Thus, Figure 20 is the optimal model.

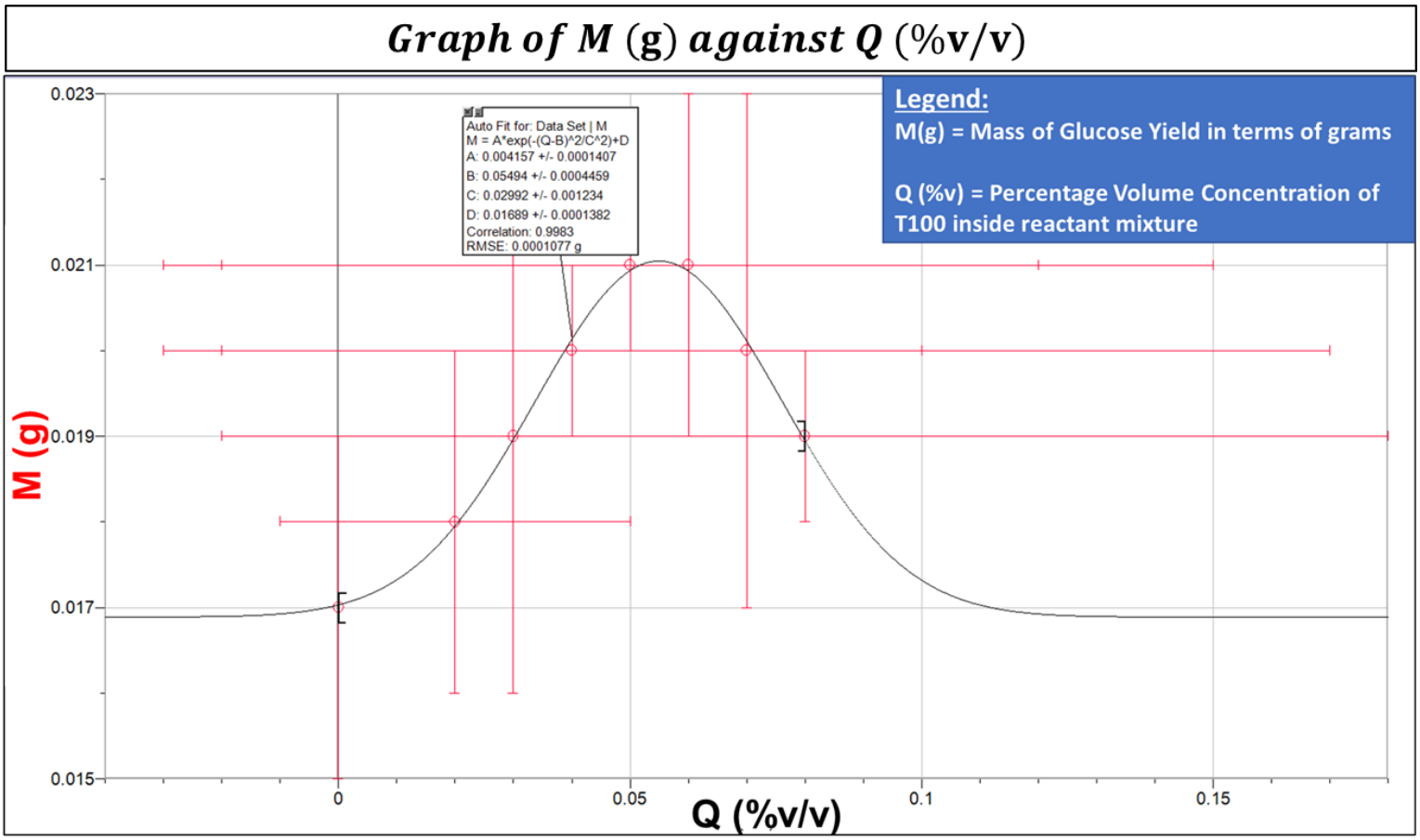

Figure 20: Gaussian Regression of M(g) against Q(%v/v)

6.2: Determining Q_{opt}

From Table 9, a curve has been plotted (Figure 20), with the equation:

$$\boldsymbol{M} = 0.00416e^{-\left(\frac{\boldsymbol{Q}-0.0549}{0.0300}\right)^2} + 0.0169$$

$$\boldsymbol{M} = mass\ of\ glucose\ yield$$

$$\boldsymbol{Q} = \%v/v\ of\ T100\ solution$$

At the curve's maximum point, glucose yield is maximising, corresponding to the experimental Q_{opt}, determined in Table 12.

For an equation $y = Ae^{-\left(\frac{x-b}{c}\right)^2} + d$, given $A, c > 0$ and $A, b, c \in \mathbb{R}$.

$$\frac{dy}{dx} = Ae^{-\left(\frac{x-b}{c}\right)^2} \times \left(\frac{2b-2x}{c^2}\right)$$

At maximum point, $\frac{dy}{dx} = 0$.

$$\text{For } x \in \mathbb{R},\ e^x > 0 \Rightarrow Ae^{-\left(\frac{x-b}{c}\right)^2} > 0$$

$$\therefore \frac{2b-2x}{c^2} = 0$$

$$\therefore x = b$$

$$\therefore Q_{opt} = 0.0549\ \%v/v$$

Table 12: Calculating Q_{opt}

6.3: Error Propagating Q_{opt}

At maximum point, $x = b$ (Table 12),

$$\therefore \frac{\Delta x}{x} = \frac{\Delta b}{b} = \frac{\Delta b}{x}$$

$$\Delta x = x\left(\frac{\Delta b}{x}\right) = \Delta b = 0.0004(1.s.f)$$

$$\Delta Q_{opt} = 0.0004(1\ s.f.)$$

Table 13: Calculating ΔQ_{opt}

6.4 Discussion

Experimental $Q_{opt} = (0.05494 \pm 0.0004)\ \%v/v$.

Literature $Q_{opt} = 0.05\ \%v/v$ (J. W. Park et al., 1992).

$$\therefore Percentage\ Error = \frac{|0.05 - 0.0549|}{0.05} \times 100\% = 10\%$$

$$\therefore Percentage\ Uncertainty = \frac{0.0004}{0.0549} \times 100\% = 0.7\%$$

The low percentage error indicates numerous experimental strengths. However, the percentage error (10%) is greater than percentage uncertainty (0.7%), suggesting the systematic errors had a greater impact than random errors.

7. Evaluation

7.1: Comparison with Literature

Comparing with the literature (J. W. Park et al., 1992)'s experiment, this experiment had a significantly lower reducing sugar concentration ($\boldsymbol{c}$). Their experiment's range was $2.3\mathrm{gL}^{-1} \leq c \leq 2.7\mathrm{gL}^{-1}$. This experiment's is $0.483\mathrm{gL}^{-1} \leq c \leq 0.681\mathrm{gL}^{-1}$, despite similar substrate mass.

This discrepancy is due to differing substrates. Their experiment's substrate is primarily lignocellulose yields more reducing sugars (glucose + xylose) (Gregory & Bolwell, 1999) than this experiment's cotton (only glucose), at same substrate mass.

Additionally, their experiment blended newspapers to extract lignocellulose, mechanically weakening lignocellulose's intermolecular bonds prior enzymatic-hydrolysis, thus increasing $\boldsymbol{c}$.

7.2: Weaknesses and Limitations

7.2.1: Dilution Titration

Prior to a change in methodology, a $10\%v/v$ T100 diluted solution was prepared instead of $0.01\%v/v$. Therefore, to reuse the solution, dilution titration was performed. However, after a week's storage, in the overly concentrated $10\%v/v$ solution, despite shaking vigorously, or using magnetic stirrers and magnetic stir plate, some of the T100 remained settled at the bottom of the volumetric flask, indicating a lack of homogeneity in the solution.

Consequently, the diluted $0.01\%v/v$ T100 solution was lower concentration than expected, meaning the reactant mixtures contained lesser T100 than anticipated. But, interpreting its impact on glucose yield is impossible without further information (Figure 21); ***random error***.

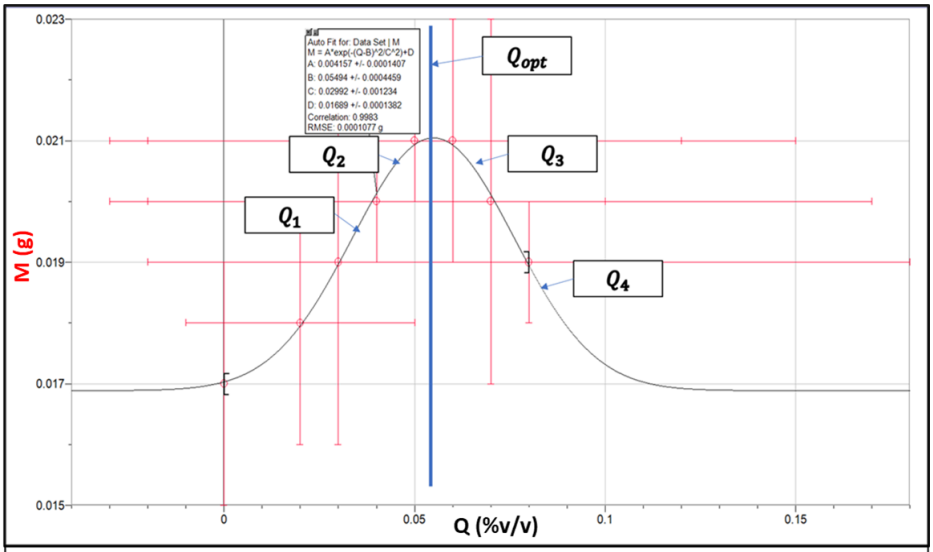

Comparing Q_1 and Q_3	
As Q_1 increases to Q_2, M also increases.	As Q_3 increases to Q_4, M decreases.
As Q_1 increases to Q_4, M decreases.	
Therefore, the impact of increasing Q on yield is uncertain, unless information about initial Q and how much Q increases is provided.	

Figure 21: Change in Q yields an undeterminable impact on M

Improvement

A simple method is heating the volumetric flask (Z. Wang et al., 2008) at moderate temperatures, since increased temperatures increase T100's water-solubility. However, this approach's effectiveness depends on Krafft Point – the temperature threshold beyond which surfactants' water-solubility plateaus (Figure 22).

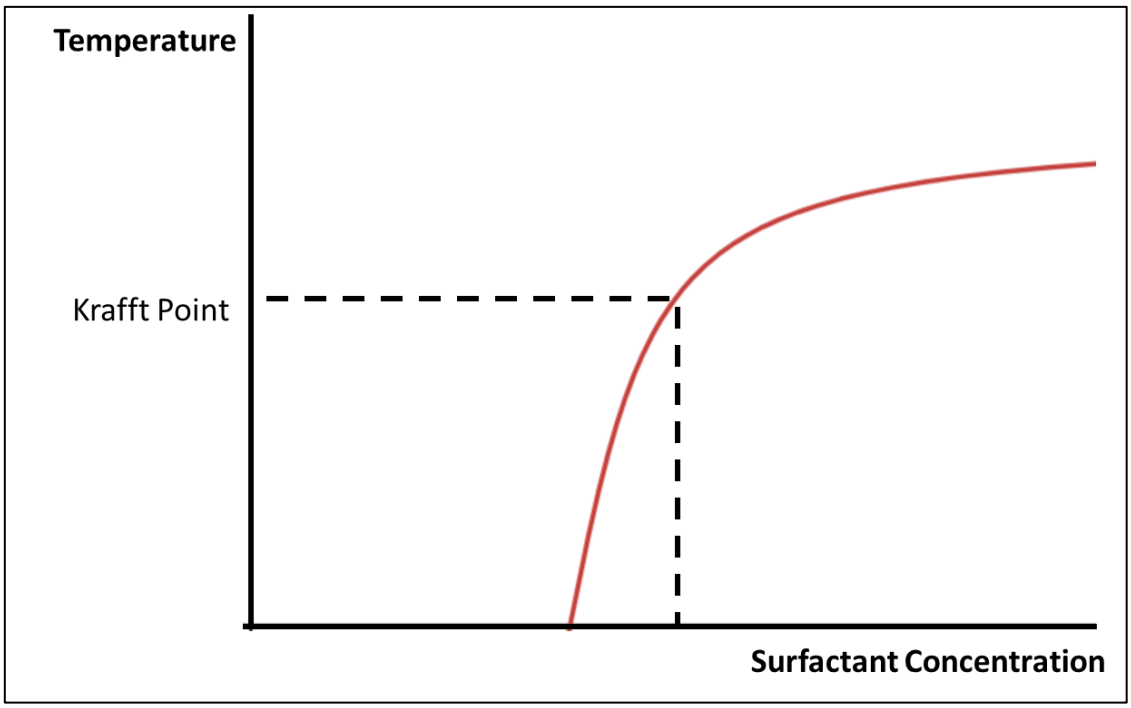

Figure 22: Krafft Point (Z. Wang et al., 2008)

Extensive literature only revealed T100's Krafft Point is within $0 - 100℃$; not an exact value (Z. Wang et al., 2008). Therefore, if its Krafft Point is at room-temperature, this error does not rectify as maximum solubility is achieved.

Nevertheless, sonication is another complex alternative. It is widely used to solubilise gels (like the settled T100 solution), by directing ultrasonic waves to T100's concentrated solution, helping dispersing T100 and solubilising it within water (Nascentes et al., 2001).

7.2.2: Long Experimental Process

Due to time constraints per lab session, reactant mixtures (pH6 buffer and T100 solution) were prepared in advance. However, despite being sealed with parafilm, water within the pH6 buffer might have evaporated between preparation and use in the reaction, increasing $\boldsymbol{Q}$ across all experiments.

However, determining its impact on $\boldsymbol{M}$ is complicated (Figure 21); **random error**.

7.2.3: Inefficient DNSA Assay

For DNSA Assay to work, DNSA must be reduced, which only occurs in alkaline environments. Therefore, 3mL NaOH (2M) was added to the DNSA assay which hydrolyses glucose, reducing glucose concentration within the assay, lowering glucose yield than its true value – a **systematic error.**

Thus, all trials registered a lower glucose yield, than its true value (Figure 23).

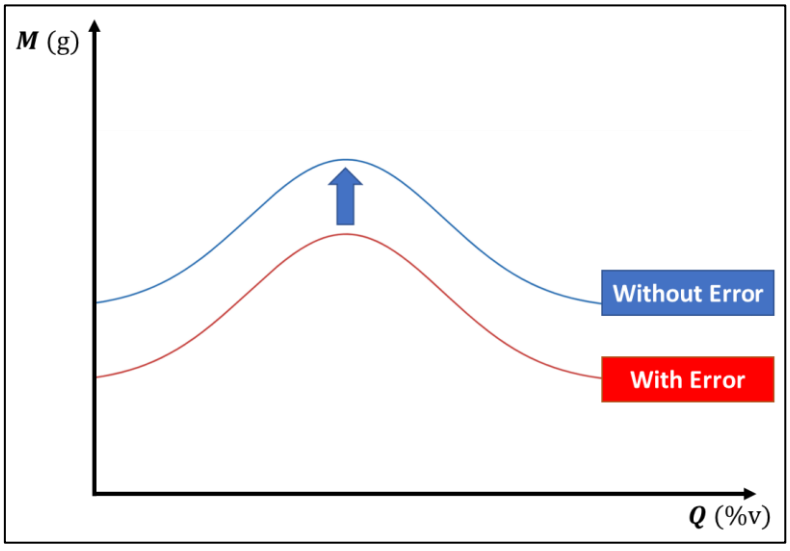

Figure 23: Graph without systematic error in DNSA Assay

Improvement

High-Performance Liquid Chromatography (HPLC) is a more accurate method to determine glucose-yield concentration (Figure 24) (Shimadzu, n.d.). But this was not considered in this experiment so as to ensure similarity with literature (J. W. Park et al., 1992), and also because required equipment were unavailable in school-laboratory.

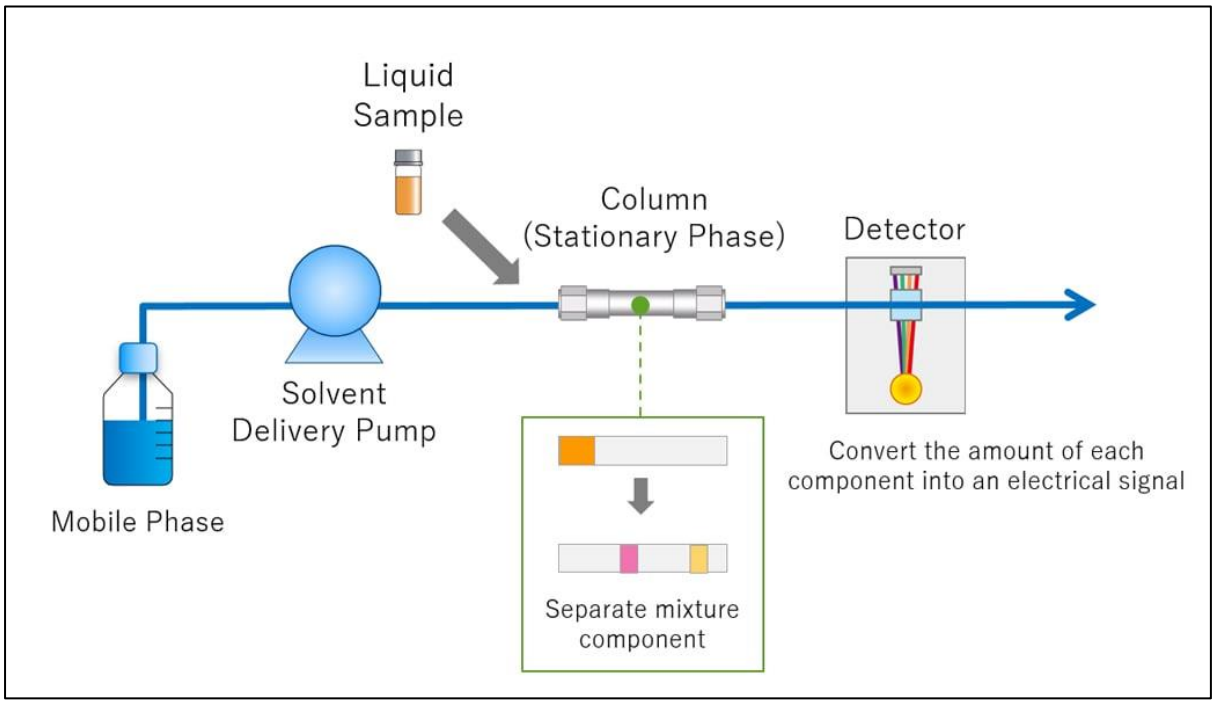

Figure 24: HPLC (Shimadzu, n.d.)

7.3: Strengths

7.3.1: Comparing Glucose Yield in terms of mass, not concentration

Glucose yield was measured in terms of mass, rather than concentration (Page 20). This avoids the issue of varying evaporation rates during heating process, preventing false representation of glucose yield, mitigating **random error**.

7.3.2: Centrifugation

Cotton substrate used is impure, evident from the black-coloured impurities after cellulose-hydrolysis (Figure 25), which interferes with DNSA assay. To remove them, filtration was not considered in case the impurities were fine enough to pass through the filter-paper. Thus, centrifugation was used, forcing impurities to sediment. Consequently, reaction mixture's supernatant was used for DNS assay, mitigating potential **random error**.

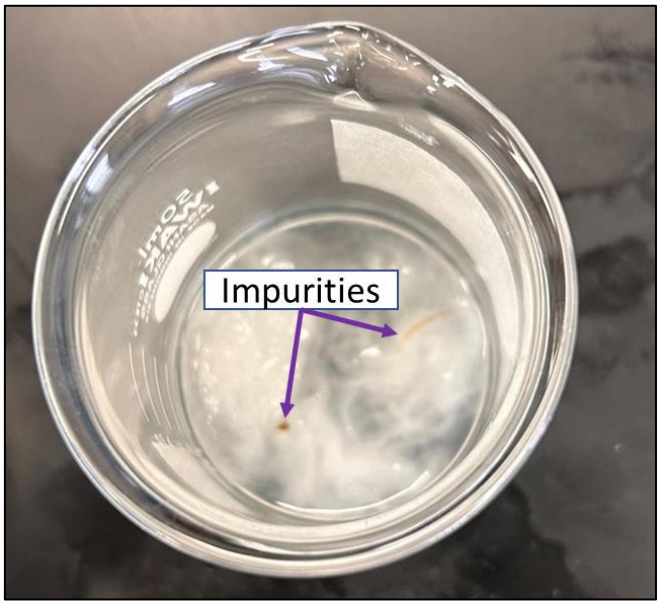

Figure 25: Impurities in Reaction Mixture

These strengths mitigated random errors, reducing percentage uncertainty to only 0.7%.

8. Conclusion

T100's $'\%v/v'$ (Q) was varied from $0\%v/v$ to $0.08\%v/v$ for cellulase-mediated cotton-hydrolysis. Then, glucose yield was determined from its DNSA Assay with spectrophotometric analysis, at each Q, revealing experimental Q_{opt} of $0.0549\%v/v$. For $Q > Q_{opt}$, glucose yield decreases at a decreasing rate, perfectly mirroring the findings by (J. W. Park et al., 1992), illustrating the outlined theory in pages 11-13.

Therefore, the hypothesis *"As T100 concentration increases from 0%v/v to 0.05%v/v (optimal concentration), glucose yield increases, beyond which glucose yield decreases at a decreasing rate"* is **validated**, given the percentage error of just 10%.

Thus, the Research Question *"How does the concentration of Triton X-100 (0%, 0.02%, 0.03%, 0.04%, 0.05%, 0.06%, 0.07%, 0.08% v/v) influence glucose yield from a 48-hour cellulase-mediated cotton-hydrolysis, quantified by DNSA assay?"* is **answered**.

8.1: Extension

There were some unresolved questions in this experiment, mainly the rationale behind using cellulase (sourced from Aspergillus Niger). It was only used given its availability. However, other cellulase types can have differing catalytic rates (Bilal et al., 2014), and should be investigated into.

(Vasilescu et al., 2022) reports magnetic cellulase having greater catalytic efficiency than the used cellulase. Thus, it can be used to increase glucose yield.

This is relevant because experimental glucose yield was very low at only $\frac{0.021}{0.950} \times 100\% = 2.21\%$.

9. Bibliography

31836001.pdf. (n.d.). Retrieved 11 April 2024, from http://www.ulab360.com/files/prod/manuals/201208/13/31836001.pdf

Abbas, M., & Li, Q. (2022, February). *(PDF) Functional characterization of cellulose synthase genes in secondary wall thickening of xylem cells during wood formation in Populus trichocarpa*. https://www.researchgate.net/publication/358734257_Functional_characterization_of_cellulose_synthase_genes_in_secondary_wall_thickening_of_xylem_cells_during_wood_formation_in_Populus_trichocarpa?_tp=eyJjb250ZXh0Ijp7ImZpcnN0UGFnZSI6Il9kaXJlY3QiLCJwYWdlIjoiX2RpcmVjdCJ9fQ

Alonso-Riaño, P., Illera, A. E., Benito-Román, O., Melgosa, R., Bermejo-López, A., Beltrán, S., & Sanz, M. T. (2024). Degradation kinetics of sugars (glucose and xylose), amino acids (proline and aspartic acid) and their binary mixtures in subcritical water: Effect of Maillard reaction. *Food Chemistry*, *442*, 138421. https://doi.org/10.1016/j.foodchem.2024.138421

Ashenhurst, J. (2017, August 17). What is Mutarotation? *Master Organic Chemistry*. https://www.masterorganicchemistry.com/2017/08/17/mutarotation/

Bilal, T., Garg, S., Singh, J., Vyas, A., Kumar, M., Gaur, N., Bala, M., Rehman, R., Varma, A., Kumar, V., & Kumar, M. (2014). Characterization of Actinomycetes and Trichoderma spp. For cellulase production utilizing crude substrates by response surface methodology. *SpringerPlus*, *3*. https://doi.org/10.1186/2193-1801-3-622

Block, G. (n.d.). *The effect of substrate concentration on enzyme activity*. Retrieved 11 April 2024, from https://www.ucl.ac.uk/~ucbcdab/enzass/substrate.htm

Burns, F., & Themens. (2014, January). *(PDF) Assessment of phosphonium ionic liquid-dimethylformamide mixtures for dissolution of cellulose*. https://www.researchgate.net/publication/259564650_Assessment_of_phosphonium_ionic_liquid-dimethylformamide_mixtures_for_dissolution_of_cellulose

Chin, M., & Somasundaran, P. (2014). Enzyme activity and structural dynamics linked to micelle formation: A fluorescence anisotropy and ESR study. *Photochemistry and Photobiology*, *90*(2), 455–462. https://doi.org/10.1111/php.12207

Clark, J. (2013a, October 3). *The Beer-Lambert Law*. Chemistry LibreTexts. https://chem.libretexts.org/Bookshelves/Physical_and_Theoretical_Chemistry_Textbook_Maps/Supplemental_Modules_(Physical_and_Theoretical_Chemistry)/Spectroscopy/Electronic_Spectroscopy/Electronic_Spectroscopy_Basics/The_Beer-Lambert_Law

Clark, J. (2013b, October 3). *The Hydrolysis of Esters*. Chemistry LibreTexts. https://chem.libretexts.org/Bookshelves/Organic_Chemistry/Supplemental_Modules_(Organic_Chemistry)/Esters/Reactivity_of_Esters/The_Hydrolysis_of_Esters

Costa, C., Viana, A., Silva, C., Marques, E. F., & Azoia, N. G. (2022). Recycling of textile wastes, by acid hydrolysis, into new cellulosic raw materials. *Waste Management*, *153*, 99–109. https://doi.org/10.1016/j.wasman.2022.08.019

DNSAinstructions.pdf. (n.d.). Retrieved 11 April 2024, from https://www.ncbe.reading.ac.uk/wp-content/uploads/sites/16/2021/10/DNSAinstructions.pdf

El-Sersy, N., Abd-Elnaby, H., Abou-Elela, G., Ibrahim, H., & El-Toukhy, N. (2010). Optimization, economization and characterization of cellulase produced by marine Streptomyces ruber. *African Journal of Biotechnology*, *9*, 6355–6364.

Felgenhauer, C., & Khudhir, M. (n.d.). *Hydrogen Bonding in Water: Properties & Importance*. StudySmarter UK. Retrieved 10 April 2024, from https://www.studysmarter.co.uk/explanations/biology/chemistry-of-life/hydrogen-bonding-in-water/

Ghosh, S., Ray, A., & Pramanik, N. (2020). Self-assembly of surfactants: An overview on general aspects of amphiphiles. *Biophysical Chemistry*, *265*, 106429. https://doi.org/10.1016/j.bpc.2020.106429

Greenwood, J. C. (2014). Chapter 1—Unleashing the Promise of Biotechnology to Help Heal, Fuel, and Feed the World. In C. Shimasaki (Ed.), *Biotechnology Entrepreneurship* (pp. 3–13). Academic Press. https://doi.org/10.1016/B978-0-12-404730-3.00001-4

Gregory, A., & Bolwell, G. P. (1999). 3.17—Hemicelluloses. In S. D. Barton, K. Nakanishi, & O. Meth-Cohn (Eds.), *Comprehensive Natural Products Chemistry* (pp. 599–615). Pergamon. https://doi.org/10.1016/B978-0-08-091283-7.00084-9

Gubitosi, M., Nosrati, P., Koder Hamid, M., Kuczera, S., Behrens, M. A., Johansson, E. G., & Olsson, U. (2017). Stable, metastable and unstable cellulose solutions. *Royal Society Open Science*, *4*(8), 170487. https://doi.org/10.1098/rsos.170487

Hussain, T. (2023, October 28). *(10) 3 Methods of Textile Recycling | LinkedIn*. https://www.linkedin.com/pulse/3-methods-textile-recycling-dr-tanveer-hussain-gzkdf/

Kong-Win Chang, J., Duret, X., Berberi, V., Zahedi-Niaki, H., & Lavoie, J.-M. (2018). Two-Step Thermochemical Cellulose Hydrolysis With Partial Neutralization for Glucose Production. *Frontiers in Chemistry*, *6*. https://doi.org/10.3389/fchem.2018.00117

Koshland, D. (n.d.). *Induced-fit theory | Description, Enzyme, Allosteric Site, & Catalysis | Britannica*. Retrieved 10 April 2024, from https://www.britannica.com/science/induced-fit-theory

Law, V. (2024, February 16). *UNDERSTANDING CURRENT APPROACHES FOR TEXTILE RECYCLING TO BETTER MANAGE FAST FASHION WASTE | NOT JUST A LABEL*. https://www.notjustalabel.com/editorial/understanding-current-approaches-textile-recycling-better-manage-fast-fashion-waste

Lefers, M. (2004, July 26). *Hydrolysis definition*. https://groups.molbiosci.northwestern.edu/holmgren/Glossary/Definitions/Def-H/hydrolysis.html

Liang, D., Liu, W., Liu, H., Wolcott, M., Dhanadapani, R., Li, H., & Wang, J. (2023, February 7). *Nanocellulose reinforced lightweight composites produced from cotton waste via integrated nanofibrillation and compounding | Scientific Reports*. https://www.nature.com/articles/s41598-023-29335-z

Lindman, B., Medronho, B., Alves, L., Norgren, M., & Nordenskiöld, L. (2021). Hydrophobic interactions control the self-assembly of DNA and cellulose. *Quarterly Reviews of Biophysics*, *54*, e3. https://doi.org/10.1017/S0033583521000019

Mekala, N. K., Potumarthi, R., Baadhe, R. R., & Gupta, V. K. (2014). Chapter 1 - Current Bioenergy Researches: Strengths and Future Challenges. In V. K. Gupta, M. G. Tuohy, C. P. Kubicek, J. Saddler, & F. Xu (Eds.), *Bioenergy Research: Advances and Applications* (pp. 1–21). Elsevier. https://doi.org/10.1016/B978-0-444-59561-4.00001-2

Metsola, R. (2020, December 29). *The impact of textile production and waste on the environment (infographics)*. Topics | European Parliament.

https://www.europarl.europa.eu/topics/en/article/20201208STO93327/the-impact-of-textile-production-and-waste-on-the-environment-infographics

MSDS-35DINITROSALICYLIC-ACID-CASNO-609-99-03481-EN.pdf. (n.d.). Retrieved 11 April 2024, from https://www.lobachemie.com/lab-chemical-msds/MSDS-35DINITROSALICYLIC-ACID-CASNO-609-99-03481-EN.aspx

NCMC. (n.d.). *Principle of Surface Tension Reduction by Surfactants*. Nanjing Chemical Material Corp. Retrieved 10 April 2024, from https://www.njchm.com

octet-sodium-acetate-buffers-datasheet-18-1068-18-1069-18-1070-en-uk-l-sartorius-pdf-137254—Data.pdf. (n.d.). Retrieved 11 April 2024, from https://www.sartorius.com/download/1138332/octet-sodium-acetate-buffers-datasheet-18-1068-18-1069-18-1070-en-uk-l-sartorius-pdf-137254--data.pdf

Pardo, A. G., & Forchiassin, F. (1999). Influence of temperature and pH on cellulase activity and stability in Nectria catalinensis. *Revista Argentina De Microbiologia*, *31*(1), Article 1.

Park, J. W., Takahata, Y., Kajiuchi, T., & Akehata, T. (1992). Effects of nonionic surfactant on enzymatic hydrolysis of used newspaper. *Biotechnology and Bioengineering*, *39*(1), 117–120. https://doi.org/10.1002/bit.260390117

Park, S., Mun, S., & Kim, Y.-R. (2020). Influences of added surfactants on the water solubility and antibacterial activity of rosemary extract. *Food Science and Biotechnology*, *29*(10), 1373–1380. https://doi.org/10.1007/s10068-020-00792-w

Pedersen, J. N., Pérez, B., & Guo, Z. (2019). Stability of cellulase in ionic liquids: Correlations between enzyme activity and COSMO-RS descriptors. *Scientific Reports*, *9*(1), 17479. https://doi.org/10.1038/s41598-019-53523-5

Robinson, P. K. (2015). Enzymes: Principles and biotechnological applications. *Essays in Biochemistry*, *59*, 1–41. https://doi.org/10.1042/bse0590001

Sanchez, A. (2023, September 27). *(10) The Shocking Statistics of Textile Waste: Time to Take Action | LinkedIn*. https://www.linkedin.com/pulse/shocking-statistics-textile-waste-time-take-action-sanchez-dmin/

Sánchez-Muñoz, S., Balbino, T. R., de Oliveira, F., Rocha, T. M., Barbosa, F. G., Vélez-Mercado, M. I., Marcelino, P. R. F., Antunes, F. A. F., Moraes, E. J. C., dos Santos, J. C., & da Silva, S. S. (2022). Surfactants, Biosurfactants, and Non-Catalytic Proteins as Key Molecules to Enhance Enzymatic Hydrolysis of Lignocellulosic Biomass. *Molecules*, *27*(23), 8180. https://doi.org/10.3390/molecules27238180

SDB-9356-IE-EN.pdf. (n.d.). Retrieved 11 April 2024, from https://www.carlroth.com/medias/SDB-9356-IE-EN.pdf?context=bWFzdGVyfHNlY3VyaXR5RGF0YXNoZWV0c3wyOTE0NDZ8YXBwbGljYXRpb24vcGRmfHNlY3VyaXR5RGF0YXNoZWV0cy9oMmIvaGIwLzkwNjk5NTczMTY2MzgucGRmfGIyZWExNjc1MzNmNjI1YTBlMjU4ZDUxOTBlNjIxZDg0Mjk5Mjk0YmM2ZmU0YzZhNzk5MzhiYmJjNjBmMDRiZTE

Shah, R. (2024, January). *Global Fast Fashion Market Size & Share Analysis—Industry Research Report—Growth Trends*. https://www.coherentmarketinsights.com/industry-reports/global-fast-fashion-market

Shimadzu, G. (n.d.). *What is HPLC (High Performance Liquid Chromatography)?*. Retrieved 12 April 2024, from https://www.shimadzu.com/an/service-support/technical-support/analysis-basics/basic/what_is_hplc.html

Steilemann, M. (2023, May 16). Chemical recycling • Plastics Europe. *Plastics Europe*. https://plasticseurope.org/sustainability/circularity/recycling/chemical-recycling/

Swatloski, R. P., Spear, S. K., Holbrey, J. D., & Rogers, R. D. (2002). Dissolution of cellulose [correction of cellose] with ionic liquids. *Journal of the American Chemical Society*, *124*(18), 4974–4975. https://doi.org/10.1021/ja025790m

T8532pis.pdf. (n.d.). Retrieved 11 April 2024, from https://www.sigmaaldrich.com/deepweb/assets/sigmaaldrich/product/documents/160/855/t8532pis.pdf

Taherzadeh, M. (2009, December 31). *Textile wastes to ethanol and biogas—University of Borås*. https://www.hb.se/en/research/research-portal/projects/textile-wastes-to-ethanol-and-biogas/

Vasilescu, C., Marc, S., Hulka, I., & Paul, C. (2022). Enhancement of the Catalytic Performance and Operational Stability of Sol-Gel-Entrapped Cellulase by Tailoring the Matrix Structure and Properties. *Gels*, *8*(10), 626. https://doi.org/10.3390/gels8100626

Wang, M., Lee, U., Kwon, H., & Xu, H. (2021). *Life-Cycle Greenhouse Gas Emission Reductions of Ethanol with the GREET Model*.

Wang, Z., Lan, T., & Zhu, J. (2013). Lignosulfonate and elevated pH can enhance enzymatic saccharification of lignocelluloses. *Biotechnology for Biofuels*, *6*, 9. https://doi.org/10.1186/1754-6834-6-9

Wang, Z., Xu, J.-H., Zhang, W., Zhuang, B., & Qi, H. (2008). Cloud point of nonionic surfactant Triton X-45 in aqueous solution. *Colloids and Surfaces. B, Biointerfaces*, *61*, 118–122. https://doi.org/10.1016/j.colsurfb.2007.07.013

Wu, S., Shi, S., Liu, R., Wang, C., Li, J., & Han, L. (2023). The transformations of cellulose after concentrated sulfuric acid treatment and its impact on the enzymatic saccharification. *Biotechnology for Biofuels and Bioproducts*, *16*, 36. https://doi.org/10.1186/s13068-023-02293-4

Yang, G., Luo, X., & Shuai, L. (2021). Bioinspired Cellulase-Mimetic Solid Acid Catalysts for Cellulose Hydrolysis. *Frontiers in Bioengineering and Biotechnology*, *9*, 770027. https://doi.org/10.3389/fbioe.2021.770027

Zhang, J., & Yu, Y. (2017). Study on the Interaction Between Cellulase and Surfactants. *Tenside Surfactants Detergents*, *54*(3), 206–213. https://doi.org/10.3139/113.110493

Zhang, P., Hai, H., Sun, D., Yuan, W., Liu, W., Ding, R., Teng, M., Ma, L., Tian, J., & Chen, C. (2019). A high throughput method for total alcohol determination in fermentation broths. *BMC Biotechnology*, *19*. https://doi.org/10.1186/s12896-019-0525-7

Zuppolini, S., Salama, A., Cruz-Maya, I., Guarino, V., & Borriello, A. (2022). Cellulose Amphiphilic Materials: Chemistry, Process and Applications. *Pharmaceutics*, *14*(2). https://doi.org/10.3390/pharmaceutics14020386